Low Temperature Physics

Analysis of fluctuation conductivity in $Y_{1-x}Cd_xBa_2Cu_3O_{7-\delta}$ ($x = 0-0.4$)

Cite as: Low Temp. Phys. **46**, 901 (2020); https://doi.org/10.1063/10.0001712
Submitted: 22 July 2020 . Published Online: 30 September 2020

V. M. Aliyev, R. I. Selim-zade, J. A. Ragimov, L. V. Omelchenko, and E. V. Petrenko

Low Temperature Physics ARTICLE scitation.org/journal/ltp

Analysis of fluctuation conductivity in $Y_{1-x}Cd_xBa_2Cu_3O_{7-\delta}$ ($x = 0-0.4$)

Cite as: Fiz. Nizk. Temp. **46**, 1068–1077 (September 2020); doi: 10.1063/10.0001712
Submitted: 22 July 2020

V. M. Aliyev,[1,a)] R. I. Selim-zade,[1] J. A. Ragimov,[2] L. V. Omelchenko,[3] and E. V. Petrenko[3]

AFFILIATIONS

[1]Institute of Physics, Azerbaijan National Academy of Sciences, Baku 1143, Azerbaijan
[2]Azerbaijan Medical University, Baku 1022, Azerbaijan
[3]B. Verkin Institute of Low Temperature Physics and Engineering, National Academy of Sciences of Ukraine, Kharkov 61103, Ukraine

[a)]**Author to whom correspondence should be addressed:** v_aliev@bk.ru

ABSTRACT

The effect that the partial substitution of Cd for Y has on the mechanism of excess conductivity formation in polycrystalline $Y_{1-x}Cd_xBa_2Cu_3O_{7-\delta}$ with $x = 0$ (Y1), 0.1 (Y2), 0.3 (Y3), and 0.4 (Y4) is investigated. The resistivity ρ of the samples increases markedly with increasing x, and the critical temperature of the superconducting (SC) state transition, T_c, decreases. The mechanism responsible for the formation of fluctuation conductivity, $\sigma'(T)$, is considered within the framework of the Aslamazov–Larkin theory near T_c. The Ginzburg temperature (T_G), the critical temperature in the mean-field approximation (T_c^{mf}), the temperature of the 3D–2D crossover (T_0), and T_{01}, which limits the region of the SC fluctuations from above, are determined. It is shown that doping with Cd at $x = 0-0.4$ increases the coherence length along the c axis, $\xi_c(0)$, by 2.7 times, and the distance between the CuO_2 planes, d_{01}, by 2.2 times. The temperature dependences of the pseudogap (PG), $\Delta^*(T)$, are determined by analyzing the excess conductivity within the framework of the local pair model. It is found that with an increase in substitution, the maximum value of the PG $\Delta^*(T_{pair})$ decreases from 250.2 to 215.7 K, while the real value of the PG, measured at T_G,$\Delta^*(T_G)$, increases from 217.4 to 224.2 K.

1. INTRODUCTION

The anomalous properties of layered metal oxide high-temperature superconductors (HTSC) are one of the most important problems in modern solid-state physics.[1] In experiments on the charge transfer dynamics in such systems, a number of objective difficulties arise, including the rather complex crystal structure of HTSCs,[2,3] the nonuniform distribution of structural defects,[4] the presence of intergrain boundaries and cluster inclusions,[5] and the inhomogeneity of specific experimental samples,[6] which is often caused by different technological prehistories, etc. The physical properties of HTSCs are also unusual, especially in the normal state, where a pseudogap (PG) opens along the excitation spectrum at the characteristic temperature $T >> T_c$[7–10] (T_c is the critical temperature of the superconducting (SC) transition). It is believed that the correct understanding PG physics, which remains one of the most intriguing properties of cuprates,[11,12] will shed light on the SC pairing mechanism in HTSCs.

Since the discovery of HTSCs with active plane CuO_2 (cuprates), attempts have been made to improve their superconducting characteristics by isomorphic substitutions of one of the components.[13–20] One of the most interesting materials for studying the properties of HTSCs is the $YBa_2Cu_3O_{7-\delta}$ (YBCO) compound, because it is possible to widely vary its composition by replacing yttrium with its isoelectronic analogues, or by changing the degree of oxygen non-stoichiometry. In YBCO, yttrium is replaced by a majority of lanthanides and other elements,[1,21–30] which usually does not lead to the deterioration of the compound's superconducting properties. Pr is an exception, since PrBCO is an insulator.[31,32]

It is well-known that ions of rare earth elements and K replace yttrium atoms. Accordingly, Sr is incorporated into the positions of Ba atoms, while other dopants are incorporated into the Cu(1) position.[33] However, this process is not well understood. The mechanisms of how a modification impacts the properties of HTSCs in underdoped and overdoped regimes remain unclear, which is important since fulfilling the conditions of these regimes is necessary to achieving the optimal properties of HTSC materials. The effect of substitution on fluctuation processes and the PG is, likewise, poorly understood. Therefore, the study of substitution in

the classical structure of $YBa_2Cu_3O_{7-\delta}$ provides new data on the mechanism of superconductivity and the contribution made to superconductivity by Y, Ba, and Cu atoms.

HTSC materials are synthesized with partial substitution of Cd for Y in $YBa_2Cu_3O_x$, because despite the fact that yttrium and cadmium are heterovalent, their ionic radii are similar (0.90 and 0.95 Å, respectively). This serves as the basis for such a substitution in YBaCuO.

The goal of this study is to investigate how possible defects and structural changes impact the physical parameters, fluctuation characteristics, and PG after substituting Cd into $Y_{1-x}Cd_xBa_2Cu_3O_{7-\delta}$. Four samples of $Y_{1-x}Cd_xBa_2Cu_3O_{7-\delta}$ with $x = 0$ (Y1), 0.1 (Y2), 0.3 (Y3), and 0.4 (Y4) are considered. The resistivity of the samples increases with an increase in Cd content, especially sharply at $x = 0.3$, whereas T_c decreases nonmonotonically. The fluctuation conductivity (FLC) is analyzed within the framework of the Aslamazov–Larkin (AL) and Hikami–Larkin (CL) theories.[34,35] Near T_c, the FLC of all samples, $\sigma'(T)$, is perfectly described by the three-dimensional (3D) equation of the AL theory, which is typical for HTSCs.[1,11,32] The local pair model proposed in Refs. 11, 36, and 37 is used to analyze the temperature dependence of the PG, $\Delta^*(T)$. In accordance with the phase diagram of cuprates, $\Delta^*(T)$ increases nonmonotonically with an increase in x.

2. EXPERIMENT

The $Y_{1-x}Cd_xBa_2Cu_3O_{7-\delta}$ samples are prepared in two stages.[23,28] At the first step, the initial components, which are in a stoichiometric ratio, are mixed and annealed in air at a temperature of 1120 K for 25 h. At the second step, the resulting compositions are annealed in oxygen ($P = 1.2-1.5$ atm) at a temperature of 1190 K for 25 h, and slowly cooled to room temperature. It is found that when yttrium is replaced with cadmium in the composition $Y_{1-x}Cd_xBa_2Cu_3O_{7-\delta}$ up to $x \sim 0.4$, the superconducting transition is retained at $T_c \sim 85$ K. High-resistance samples resulting from the complete substitution of Cd for Y in the $Y_{1-x}Cd_xBa_2Cu_3O_{7-\delta}$ composition are obtained, and these exhibit an SC transition at lower temperatures. In this study, we analyze the results of replacing Y with Cd up to $x = 0.4$.

Samples $8 \times 4 \times 3$ mm in size are cut from compressed tablets (12 mm diameter and 3 mm thickness) of synthesized polycrystalline material. The electrical resistance is measured according to the standard four-probe method. The current contacts are created by applying a silver paste and subsequently connecting silver conductors with 0.05 mm diameters to the ends of the polycrystalline sample, in order to ensure the current spreads across it in a uniform manner. The potential contacts located at the middle of the sample's surface are created in a similar way. Then, a three-hour annealing process is carried out at a temperature of 200 °C in an oxygen atmosphere. This procedure makes it possible to obtain a contact transition resistance of 1 Ω and to perform resistive measurements at transport currents of up to 10 mA in the *ab*-plane.

3. RESULTS AND DISCUSSION

Resistive properties

The temperature dependences of the resistivity $\rho(T) = \rho_{ab}(T)$ of the synthesized $Y_{1-x}Cd_xBa_2Cu_3O_{7-\delta}$ polycrystalline samples at $x = 0$ (Y1), 0.1 (Y2), 0.3 (Y3), and 0.4 (Y4) are shown in Fig. 1. The $\rho(T)$ dependences at different values of x have a shape characteristic of optimally doped HTSCs.[38] One exception is the nonlinear dependence $\rho(T)$ at $x = 0$, $\rho(T) \sim T^2$, which is typical for overdoped cuprates.[38] Analysis shows that the data in this case are well approximated by the equation $\rho(T) = \rho_0 + B_1T + B_2T^2$ with the parameters $\rho_0 = 9.07$, $B_1 = 0.1442$, and $B_2 = 0.0000957$, obtained by approximating data using the Origin computer program. The coefficient of the quadratic term is very small, but nonzero. Thus, we have an overdoped sample. This result is particularly interesting, since it is impossible to obtain an overdoped sample of $YBa_2Cu_3O_{7-\delta}$ simply by oxygen intercalation. The maximum that can be obtained is $\delta = 0$ and an oxygen index $7 - \delta = 7$, at $T_c \sim 92$ K.[38] It is most likely that such a dependence $\rho(T)$ is specific to this polycrystalline sample.

As seen in Fig. 1, in the considered case, the critical temperatures of the Y–Ba–Cu–O system samples remain up to ~85 K upon doping with Cd. At the same time, the resistivity $\rho(T)$ of the Y1–Y4 samples in the normal phase at 300 K increases by almost 2.5 times, in comparison with $YBa_2Cu_3O_{7-\delta}$ (Table I). In the temperature range above $T^* = (123.7 \pm 0.5)$ K (Y2), $T^* = (134.6 \pm 0.5)$ K (Y3), and $T^* = (123.3 \pm 0.5)$ K (Y4) up to 300 K, the $\rho(T)$ dependences of the doped samples are linear with a slope $d\rho/dT = 0.13$, 0.17, and 0.27 (μΩ cm)/K, respectively, for Y2, Y2, and Y3 (Fig. 1). The slope is determined by a computer approximation of the experimental dependences in the normal state, $\rho_N(T)$, which perfectly confirmed the linear course of this curve. A more accurate method for determining T^* is obtained by exploring the criterion $[\rho(T)-\rho_0]/aT = 1$, which is derived by transforming the linear equation,[39] wherein ρ_0 is the residual resistivity and the y-intercept

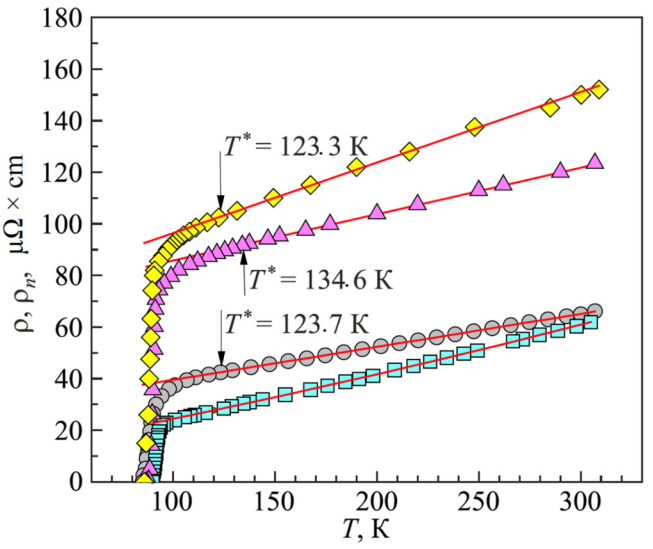

FIG. 1. ρ as a function of temperature for $Y_{1-x}Cd_xBa_2Cu_3O_{7-\delta}$ polycrystalline samples, at various cadmium concentrations x: 0 (Y1, squares); 0.1 (Y2, circles); 0.3 (Y3, triangles), and 0.4 (Y4, diamonds). The straight lines denote $\rho_N(T)$, extrapolated to the low-temperature region.

TABLE I. Parameters of the $Y_{1-x}Cd_xBa_2Cu_3O_{7-\delta}$ polycrystalline sample, obtained by analyzing the fluctuation conductivity.

YBCO (Cd)	ρ(300 K), μΩ cm	ρ(100 K), μΩ cm	T_c, K	T^{mf}_c, K	T_G, K	T_0, K	T_{01}, K	ΔT_{fl}, K	d_{01}, Å	$\xi_c(0)$, Å
Y1 ($x = 0$)	60	24	90.2	91.99	92.1	92.8	101.0	8.9	3.4	1.1
Y2 ($x = 0.1$)	65	37	84.9	88.36	88.8	90.2	100.9	12.1	4.3	1.67
Y3 ($x = 0.3$)	120	80	88.0	90.62	90.7	91.7	99.0	8.3	4.1	1.26
Y4 ($x = 0.4$)	150	92	86.7	89.06	89.7	95.0	102.6	12.9	7.4	3.0

at $T = 0$. In this case, T^* is defined as the temperature of the deviation of $\rho(T)$ from 1.[32,39]

3.2. Analysis of fluctuation conductivity

The fluctuation conductivity for all investigated samples is determined by analyzing the excess conductivity $\sigma'(T)$, which is calculated from the difference between the measured resistivity $\rho(T)$ and the linear normal resistivity of the sample $\rho_N(T) = aT + \rho_0$, extrapolated to the low-temperature region:[11,40–43]

$$\sigma'(T) = \sigma(T) - \sigma_N(T) = [1/\rho(T)] - [1/\rho_N(T)] = [\rho_N(T) - \rho(T)]/[\rho(T) - \rho_N(T)]. \quad (1)$$

As shown in Refs. 11, 40, and 43, the linear temperature dependence of the resistivity at high temperatures is a distinctive feature of the normal state of HTSC cuprates, which is characterized by the stability of the Fermi surface.[43] It is possible that the Fermi surface is rearranged below the PG opening temperature, T^*.[8,43] As a result, at $T \leq T^*$, not only are all properties of HTSCs almost entirely different and $\rho(T)$ deviates from the linear dependence,[7,40–43] but the density of charge carriers (DOS) at the Fermi level decreases,[44,45] which, by definition, is what we refer to as the PG.[1,7–12] Obviously, the resulting excess conductivity $\sigma'(T)$, determined using Eq. (1), should contain information about the temperature dependence of both the FLC and the PG.[11,32,40–43] This approach is used to analyze $\sigma'(T)$ for all values of x.

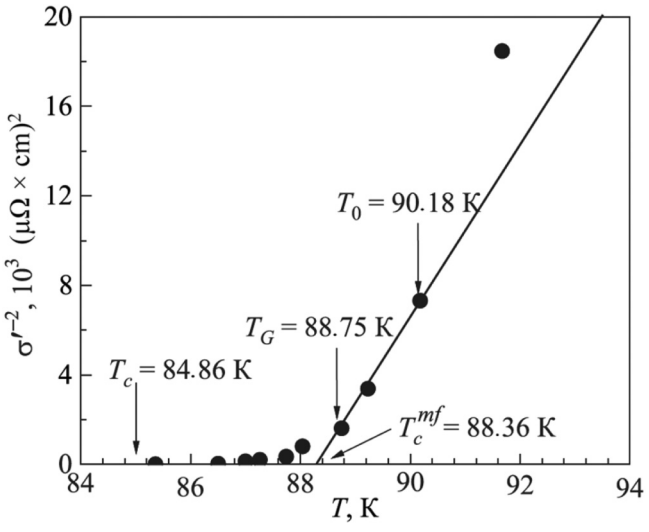

FIG. 2. The inverse square of the excess conductivity as a function of temperature $\sigma'^{-2}(T)$, for the $Y_{1-x}Cd_xBa_2Cu_3O_{7-\delta}$ polycrystalline sample at $x = 0.1$, which determines the T_c^{mf} of the Y2 sample. The arrows indicate the characteristic temperatures T_c, T_G, and T_0 (see text).

Let us consider the method for determining the FLC within the framework of the local pair (LP) model, in more detail.[11,40] First of all, it is necessary to determine the critical temperature in the mean field approximation T_c^{mf}, which separates the FLC region from the critical fluctuation region,[11,46] i.e., fluctuations of the SC order parameter Δ_0 directly near T_c (where $\Delta_0 < kT$), which are not taken into account by the Ginzburg–Landau theory.[47] T_c^{mf} is an important parameter of FLC and PG analysis, since it defines the reduced temperature

$$\varepsilon = (T/T_c^{mf} - 1), \quad (2)$$

which is included in all equations that are utilized in this study. In an HTSC near T_c, the coherence length along the c axis, $\xi_c(T) = \xi_{c0}(0)(T/T_c^{mf} - 1)^{-1/2}$, is greater than the corresponding size of the YBCO unit cell $d = c = 11.7$ Å,[33] and the fluctuation Cooper pairs (FCP) interact throughout the entire volume of the superconductor. Accordingly, this is the 3D fluctuation region. As a result, up to the temperature of the 3D–2D crossover $T_0 > T_c^{mf}$, the conductivity $\sigma'(\varepsilon)$ is always extrapolated by the fluctuation contribution of the Aslamazov–Larkin theory[34] for 3D systems:[11,40–42]

$$\sigma'_{3D-AL} = C_{3D}\frac{e^2}{32\hbar\xi_c(0)}\varepsilon^{-1/2}. \quad (3)$$

From here, we easily obtain that $\sigma'^{-2}(T) \sim \varepsilon \sim T - T_c^{mf}$. It is clear that the $\sigma'^{-2}(T)$ extrapolated by the linear dependence vanishes at $T = T_c^{mf}$,[46] as shown in Fig. 2 for the example Y2. In addition to T_c^{mf} and T_c, Fig. 2 shows T_G, which is the Ginzburg temperature up to which the mean field theories are valid with decreasing T,[47,48] and T_0, the temperature of the 3D–2D crossover, which limits the region of 3D–AL fluctuations from above.[35,49] T_c^{mf} is determined for the remaining samples (Table I) in a similar fashion.

Having determined T_c^{mf}, we plot ln σ' as a function of ln ε for all samples, as shown in Figs. 3 and 4, in order to compare the results with the fluctuation theories. As expected, it can be seen that in all cases, the FLC is perfectly approximated by the 3D-AL fluctuation contribution (3) near T_c (straight 3D–AL lines with a slope $\lambda = -1/2$). This means that the classic 3D FLC is always

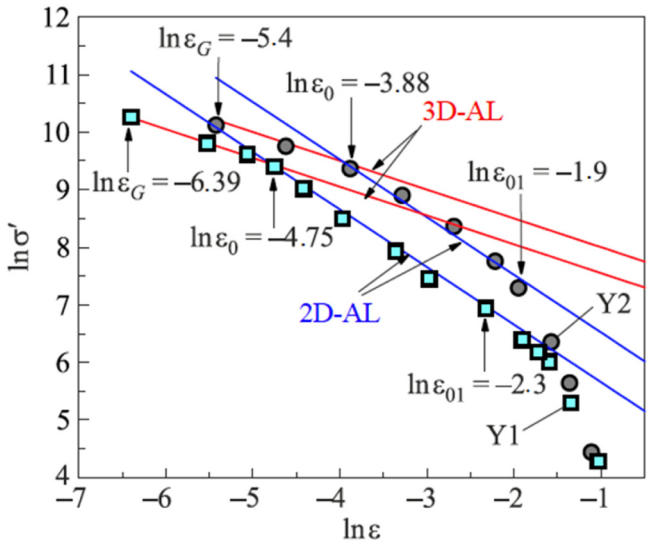

FIG. 3. Dependences of ln σ' on ln ε for the $Y_{1-x}Cd_xBa_2Cu_3O_{7-\delta}$ polycrystalline sample at $x = 0$ (Y1) and 0.1 (Y2), in comparison with the 3D–AL (3) and 2D–AL (4) fluctuation theories. ln ε_{01} determines T_{01} (Table I), which specifies the region of SC fluctuations above T_c, ln ε_0 determines the crossover temperature T_0 (Table I), and ln ε_G is the Ginzburg temperature T_G (Table I).

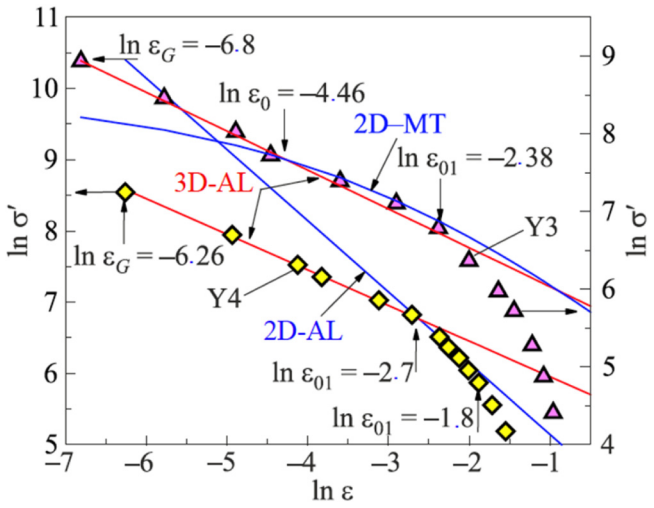

FIG. 4. Dependences of ln σ' on ln ε for the Y3 and Y4 polycrystalline samples of $Y_{1-x}Cd_xBa_2Cu_3O_{7-\delta}$, in comparison with the 3D–AL (3), 2D–AL (4), and 2D-MT (6) fluctuation theories. For clarity, the data are shifted along the *y*-axis.

realized in cuprate HTSCs, when T tends to T_c and $\xi_c(T) > d$.[11,32,40,42] Above T_0, the slope of ln σ' as a function of ln ε undergoes a sharp change. Such a dependence with a slope $\lambda = -1$ (see straight lines in Figs. 3 and 4 for Y4) is typical for 2D–AL fluctuations:[34]

$$\sigma'_{2D-AL} = C_{2D}\frac{e^2}{16\hbar d}\varepsilon^{-1}. \quad (4)$$

Thus, at the T_0 values given in Table I, there is a 3D–2D crossover. Obviously, $\xi_c(T_0) = d$, from which we get

$$\xi_c(0) = d\sqrt{\varepsilon_0}. \quad (5)$$

Knowing that $T_0 = 92.8$ K for Y1, we find $\xi_c(0) = (1.1 \pm 0.02)$ Å according to Eq. (5). The values of $\xi_c(0)$ are similarly obtained for the remaining samples, given in Table I. It can be seen that, upon doping with Cd, $\xi_c(0)$ increases to $\xi_c(0) = (3.0 \pm 0.02)$ Å at $x = 0.4$ (Y4). This is due to a noticeable increase in the region of 3D fluctuations (see Fig. 4, diamonds). At the same time, Y2 ($x = 0.2$) demonstrates the smallest $T_c = 84.9$ K, while $\xi_c(0) = (1.67 \pm 0.02)$ Å. As such, the direct relationship between the coherence length and T_c, which in the classical theory of superconductivity is given by the formula $\xi \sim \hbar v_F/\pi\Delta_0 \sim \hbar vF/k_BT_c$,[47] is not observed in this case. Here, it is taken into account that according to the Bardeen-Cooper-Schrieffer (BCS) theory,[47] $\pi\Delta_0 \sim k_BT_c$.

Above the temperature T_0, up to T_{01}, which limits the region of the SC fluctuations from above (≈101.0 K for Y1), $d > \xi_c(T) > d_{01}$ and the 3D state is lost. However, $\xi_c(T)$ still connects the inner conducting CuO_2 planes via Josephson interaction, and the distance between them is $d_{01} \approx 3.5$–4 Å.[33] It can be seen that in the samples studied above T_0, the FLC is perfectly described by the 2D–AL theory (5) (see Fig. 3), with the parameters given in Table I. Such a dependence of ln σ' on ln ε, with a short region of 3D fluctuations near T_c, is characteristic of bismuth-based HTSCs like $Bi_{1.6}Pb_{0.4}Sr_{1.8}Ca_{2.2}Cu_3O_{10}$ (Bi2223),[50] and indicates the presence of various structural defects.[1] In well-structured YBCO samples,[40] above T_0, the FLC is always described by the 2D Maki–Thompson (2D–MT) fluctuation term of the Hikami–Larkin theory:[35]

$$\sigma'_{2D-MT} = C_{2D}\frac{e^2}{8d\hbar}\frac{1}{1-\alpha/\delta}\ln\left(\frac{\delta}{\alpha}\frac{1+\alpha+\sqrt{1+\alpha}}{1+\delta+\sqrt{1+2\delta}}\right)\varepsilon^{-1}. \quad (6)$$

Here, $\alpha = 2[\xi_c(0)/d]2\varepsilon^{-1}$ is the coupling parameter;

$$\delta = 1.203(l/\xi_{ab})(16/\pi\hbar)[\xi_c(0)/d]^2k_BT\tau_\varphi \quad (7)$$

is the uncoupling parameter; τ_φ the phase relaxation time of fluctuation pairs, which is determined by the formula $\tau_\varphi\beta T = \pi\hbar/(8k_B\varepsilon_{01}) = A/\varepsilon_{01}$. The factor $\beta = 1.203(l/\xi_{ab})$, where l is the mean free path and ξ_{ab} is the coherence length in the ab plane, which takes into account the pure limit approximation.[11,40] The dependence of ln σ' on ln ε (6) is observed in sample Y3 between $T_0 = 91.7$ K (ln $\varepsilon_0 = -4.46$) and $T_{01} = 99$ K (ln $\varepsilon_{01} = -2.38$) (the MT–2D curve in Fig. 4) with the parameters given in Table I. This result indicates a possible, but somewhat unexpected, improvement in the structure of the Y3 sample ($x = 0.3$) upon doping. With a further increase in the Cd content to $x = 0.4$ (sample Y4), the FLC value noticeably decreases (Fig. 4, diamonds), and above T_0, the 2D–AL dependence (4) is restored. At the same time, the largest

region of 3D fluctuations is observed, $T_0 - T_G = 5.3$ K, which is ~7.6 times greater than that in Y1 and 5.3 times greater than that in Y3. Sample Y4 also demonstrates the largest region of SC fluctuations, $\Delta T_{fl} = T_{01} - T_G$, $\xi_c(0)$, and the value d_{01} (see Table I). It can be concluded that the content of Cd at $x \geq 0.4$ leads to noticeable distortions of the YBCO structure, which then lead to an increase in the distance between the conducting planes d_{01} by a factor of ~2.2, compared to that in undoped YBCO.

The value of d_{01} is found based on the fact that above T_{01}, the experimental data for all samples deviate from the fluctuation theory towards smaller values. Above T_{01}, the value $\xi_c(0) < d_{01}$, and all charge carriers—both fluctuation pairs and normal electrons—are inside the CuO_2 planes, which are not related by any correlation interaction.[40,49] It is obvious that $\xi_c(T_{01}) = d_{01}$, i.e., $\xi_c(0) = d_{01}\sqrt{\varepsilon_{01}}$ (5). At the same time, $\xi_c(0) = d\sqrt{\varepsilon_0}$. Based on this, using simple algebra and accounting for the fact that $d = 11.7$ Å, we get that $d_{01} = d\sqrt{\varepsilon_0/\varepsilon_{01}}$. As follows from Table I, all parameters of the samples increase nonmonotonically with an increase in the content of Cd. The only exception is the parameter d_{01}, which greatly increases at $x = 0.4$. Simultaneously, $\xi_c(0)$ also increases by ~2.7 times. Such an increase in $\xi_c(0)$ does not follow from theory, where $\xi \sim \hbar v_F/k_B T_c$,[47] since T_c changes insignificantly (see Table I). This result confirms the conclusion that it is the incorporation of Cd into the YBCO structure that leads to the noticeable increase in $\xi_c(0)$. Otherwise, it must be assumed that doping greatly increases the Fermi velocity, v_F, which is not an obvious idea and requires further study. Thus, the various defect ensembles that arise in YBCO upon doping with Cd significantly affect the behavior of HTSCs. It is assumed that the behavior of the PG temperature dependences, considered below, should also change with increasing x.

3.3. Analyzing magnitude and temperature dependence of PG

The fact that the FLC obeys classical fluctuation theories at $\Delta T_{fl} = T_{01} - T_G$ means that SC fluctuations exist up to T_{01} in HTSCs. This also suggests that the phase rigidity of the order parameter wavefunction in HTSCs is conserved until T_{01}.[51,52] That is, in this temperature range, FCPs largely behave as superconducting, but not coherent pairs (the so-called "short-range phase correlations"[11,40]), as noted above. At the same time, as follows from Table I, the temperature range in which the SC fluctuations obey the fluctuation theories, $\Delta T_{fl} \sim 13$ K above T_c, which is relatively small, whereas the range in which excess conductivity is observed for the studied samples is $T^* - T_c^{mf} \sim 40$ K. However, a rigorous theory that could describe the excess conductivity $\sigma'(T)$ over the entire temperature range from T^* to T_c^{mf} is still lacking. Therefore, the PG will be analyzed according to the approach developed in Refs. 53 and 54.

In this case, the excess conductivity $\sigma'(T)$ over the studied temperature range can be described by the following equation:

$$\sigma'(T) = A_4 \frac{e^2\left(1 - \frac{T}{T^*}\right)\exp\left(-\frac{\Delta^*}{T}\right)}{16\hbar\xi_c(0)\sqrt{2\varepsilon_{c0}^*\mathrm{sh}\left(2\frac{\varepsilon}{\varepsilon_{c0}^*}\right)}}, \quad (8)$$

which contains the PG parameter Δ^* in explicit form. In Eq. (8), $1 - T/T^*$ determines the number of pairs arising at $T \leq T^*$, and $\exp(-\Delta^*/T)$ gives the number of pairs destroyed by thermal fluctuations below T_{pair}.[11,53] Solving Eq. (7) with respect to $\Delta^*(T)$, we obtain the equation for the PG

$$\Delta^*(T) = \ln\left[A_4\left(1 - \frac{T}{T^*}\right)\frac{1}{\sigma'(\varepsilon)}\frac{1}{16\hbar\xi_c(0)}\frac{1}{\sqrt{2\varepsilon_{c0}^*\mathrm{sh}\left(2\frac{\varepsilon}{\varepsilon_{c0}^*}\right)}}\right], \quad (9)$$

where $\sigma'(\varepsilon)$ is the experimentally measured excess conductivity. Equations (8) and (9) include a number of parameters, which are also determined from the experiment[32,40] within the LP model. In addition to T_c, T^*, $\xi_c(0)$, and ε, which are obtained from resistive measurements and FLC analysis, both equations include the coefficient A_4, which has the same meaning as the C-factor in FLC theory, $\Delta^*(TG)$, and the theoretical parameter ε_{c0}^*.[53–55]

Figure 5 shows the dependence of $\ln\sigma'$ on $\ln\varepsilon$ for the Y2 sample, over the temperature range from T^* to T_G, which shows that in the interval from $T_{c01} = 94.4$ K to $T_{c02} = 106.7$ K, highlighted in the figure by arrows at $\ln\varepsilon_{c01} = -2.69$ and $\ln\varepsilon_{c02} = -1.57$, $\sigma'^{-1} \sim \exp\varepsilon$.[55] This feature turns out to be one of the main properties of most HTSCs.[11,40,53–55] As a result, in the interval $\varepsilon_{c01} < \varepsilon < \varepsilon_{c02}$ (inset in Fig. 5) $\ln\sigma'^{-1}$ is a linear function of ε with slope $\alpha^* = 12.4$, which determines the parameter $\varepsilon_{c0}^* = 1/\alpha^* \approx 0.08$[55] (Table II). This approach makes it possible to obtain reliable ε_{c0}^* values for all other samples, which are also given in Table II, and,

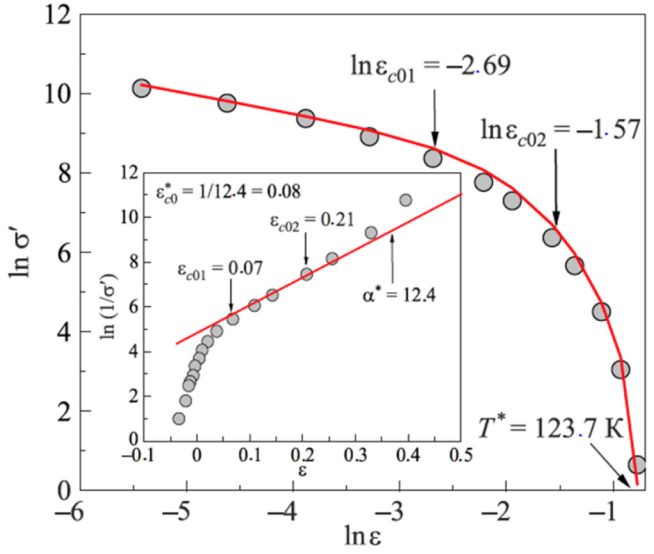

FIG. 5. Dependence of $\ln\sigma'$ on $\ln\varepsilon$ for polycrystalline Y2, plotted in the temperature range from T^* to T_G. The line shows the approximation of experimental data according to Eq. (8) with the parameters given in the text. The inset shows the dependence of $\ln(1/\sigma')$ on ε. The straight line marks a linear section, the inverse slope of which $1/\alpha^*$ determines the parameter $\varepsilon_{c0}^* = 0.08$.

TABLE II. PG analysis parameters of polycrystalline $Y_{1-x}Cd_xBa_2Cu_3O_{7-\delta}$.

YBCO (Cd)	T^*, K	A^*	$\varepsilon^*_{c0}Z$	Tpair, K	D^*, K	$\Delta^*(T_{\text{pair}})$, K	$\Delta^*(T_G)$, K
Y1 ($x = 0$)	–	–	–	–	–	–	–
Y2 ($x = 0.1$)	123.7	12.4	0.08	106.7	2.5	250.2	217.4
Y3 ($x = 0.3$)	134.6	4	0.25	125.5	2.5	234.5	223.2
Y4 ($x = 0.4$)	123.3	8	0.125	111.2	2.5	215.7	224.4

as established in Refs. 1, 32, and 40, they also noticeably affect the shape of the theoretical curves shown in Figs. 5–7 at $T >> T_{01}$; i.e., the curves are much higher than the SC fluctuation region.

Let us find the coefficient A_4, but first we will determine $\Delta^*(T_G)$, which is used in Eq. (8), by superimposing the theory onto the experimental data, which are plotted as ln σ′ as a function of $1/T$ (see Fig. 6).[56] Refs. 1, 32, and 40 show that in these coordinates, the shape of the theoretical curve turns out to be very sensitive to the value $\Delta^*(T_G)$. In addition, it is assumed that $\Delta^*(T_G) = \Delta_0(0)$, where Δ_0 is the SC gap.[57,58] We emphasize that it is the quantity $\Delta^*(T_G)$ that determines the true value of the PG, and is used to estimate the value of the BCS ratio $D^* = 2\Delta_0(0)/k_BT_c = 2\Delta^*(T_G)/K_BT_c$ in a specific HTSC sample.[1,32,40] The best approximation of ln σ′ as a function of $1/T$ by Eq. (8) for sample Y2 is achieved at $D^* = 5 \pm 0.2$. The same D^* is obtained for all samples analyzed in this study (Table II), which is a typical value for YBCO[53,54] and significantly exceeds the limit of the BCS theory for d-wave superconductors [$2\Delta_0\ (0)/k_BT_c \approx 4.28$].[59,60]

Having determined the parameters, we find the coefficient A_4. We calculate σ′(ε) according to Eq. and, having chosen A_4, superimpose the theory onto the experiment in the region of 3D–AL fluctuations near T_c, where ln σ′(ln ε) is the linear function of the reduced temperature ε with slope $\lambda = -1/2$[32,40,61] (Fig. 5). As can be seen in the figure, Eq. (8) with $\varepsilon^*_{c0} = 0.08$, $\Delta^*(T_G)/k_B = 2.5T_c \approx 213$ K, and $A_4 = 55$, provides a good description of the experiment between T^* and T_G, as expected. This fact allows us to assume that Eq. (9) gives a reliable value and temperature dependence of the PG, $\Delta^*(T)$.

The dependences $\Delta^*(T)$ are plotted according to the determined parameters, for samples Y2, Y3, and Y4. Note that no PG is observed in Y1, since the sample is in the overdoped mode. The dependence $\Delta^*(T)$ is calculated in the LP model according to Eq. (9) for Y2, with the experimentally determined $T^* = 123.7$ K, $T_c^{mf} = 88.36$ K, $\xi(0) = 1.67$ Å, $\varepsilon^*_{c0} = 0.08$, and $A_4 = 55$, as shown in Fig. 7(circles). This same dependence is plotted for Y3 with the parameters $T^* = 134.6$ K, $T_c^{mf} = 90.62$ K, $\xi_c(0) = 1.26$ Å, ε^*_{c0}=0.25, and $A_4 = 15$ (triangles). A similar dependence for Y4 is shown by diamonds in Fig. 7, with parameters $T^* = 123.3$ K, $T_c^{mf} = 89.06$ K, $\xi_c(0) = 3.0$ Å, ε^*_{c0}=0.125, and $A_4 = 40$. The shape of the dependence $\Delta^*(T)$ for Y2 is characteristic of high-quality thin YBCO films with different oxygen concentrations[1,11,53,54] and with a clearly pronounced maximum at $T_{\text{pair}} = 106.7$ K and Δ^*

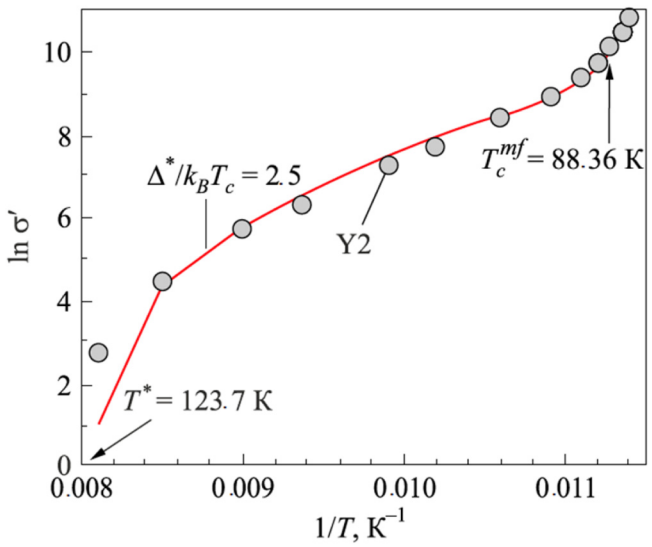

FIG. 6. ln σ′ as a function of $1/T$ (dots) for the Y2 polycrystalline sample in the temperature range from T^* to T_c^{mf} at $x = 0.1$. The line shows the data approximation according to Eq. (8) at $D^* = 2\Delta^*(T_G)/k_BT_c = 5$.

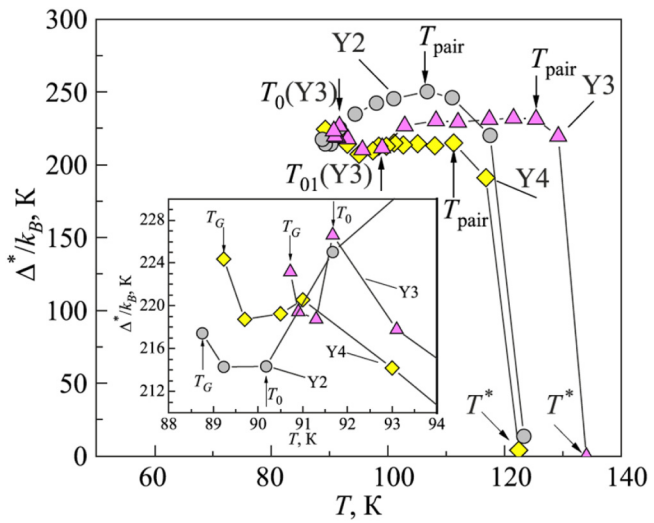

FIG. 7. Dependences $\Delta^*(T)/k_B$ for samples Y2 (circles), Y3 (triangles), and Y4 (diamonds). With an increase in the concentration of Cd, the maximum value of the PG $\Delta^*(T_{\text{pair}})$ decreases, while $\Delta^*(T_G)$ increases (see inset). Inset: the same dependences $\Delta^*(T)/k_B$ in the region of SC fluctuations near T_c.

(T_{pair}) = 250.2 K. Recall that T_{pair} is the temperature at which LPs are transformed from small-sized strongly coupled bosons that can be described as Bose–Einstein condensate (BEC), into FCPs that obey the BCS theory.[1,11,36] In other words, this is the BEC–BCS crossover temperature.[62–64] At the same time, as can be seen in the inset of Fig. 7, $\Delta^*(T)$ has a minimum at $T_0 = 90.2$ K (Table I). Conversely, in pure YBCO, the temperature T_0 usually corresponds to a maximum.[61] This indicates that defects that arise during the intercalation of Cd noticeably affect the sample properties, including those near T_c.

As the concentration of cadmium increases to $x = 0.3$ (Y3), the shape of the $\Delta^*(T)$ curve changes (Fig. 7, triangles). The $\Delta^*(T)$ maximum shifts toward higher temperatures and $T_{pair} \approx 125.5$ K, while $\Delta^*(T_{pair}) = 234.5$ K, i.e., it decreases. In the interval from T_{pair} to ~108 K, the dependence $\Delta^*(T)$ is actually linear. This shape of $\Delta^*(T)$ is characteristic of optimally doped YBCO single crystals.[65] At the same time, the shape of $\Delta^*(T)$ near T_c is the same as that of other HTSCs: at $T_{01} \sim 99$ K, a minimum is clearly observed, and at $T_0 = 91.7$ (Table I), there is a maximum at $\Delta^*(T)$ (Fig. 7 and inset). Also, the true value of the PG, $\Delta^*(T)/k_B$, increases from 217.4 K (Y2) to 223.2 K (Y3). This result allows us to conclude that sample Y3 most likely has a minimum number of defects, which is also supported by the detection of the 2D–MT fluctuation contribution along the dependence of ln σ' on ln ε (Fig. 4). With a further increase in the cadmium concentration to $x = 0.4$ (Y4), the shape of the $\Delta^*(T)$ curve (Fig. 7, diamonds) changes again. At the same time, the temperatures T^*, T_{pair}, and $\Delta^*(T_{pair})$ decrease noticeably (Table II), and the maximum at T_0 and the minimum at T_{01} disappear, which is clearly seen in Fig. 8. In fact, everything becomes the opposite: a maximum is observed at $T_{01} = 102.6$ K, and at $T_0 = 95$ K, there is a pronounced minimum, indicating an increase in the effect of defects. At the same time, $\Delta^*(T)/k_B$ increases to ~224.4 K (Table II). Ref. 66 reported a significant increase in $\Delta^*(T_G)/k_B$ under pressure in $Y_{0.95}Pr_{0.05}Ba_2Cu_3O_{7-\delta}$ single crystals, containing defects in the form of PrBCO dielectric cells. Similarly, it can be assumed that doping with Cd creates internal pressure in YBCO due to structural defects. This idea is supported by the sharp increase in the distance d_{01} between the conducting CuO_2 planes, determined from FLC analysis. Table I shows that d_{01} increases by almost 2.2 times with an increase in the Cd content from $x = 0$ to 0.4. Thus, various defect ensembles resulting from the intercalation of Cd significantly affect the properties of the studied $Y_{1-x}Cd_xBa_2Cu_3O_{7-\delta}$ polycrystalline samples.

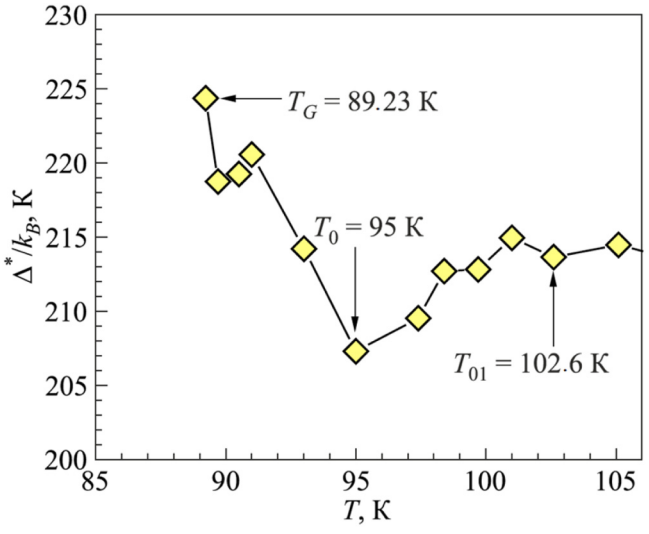

FIG. 8. Dependence $\Delta^*(T)/k_B$ for sample Y4 in the region of SC fluctuations near T_c. The arrows indicate the characteristic temperatures T_{01}, T_0, and T_G.

4. CONCLUSION

We studied the impact that partial substitution of Cd for Y has on the mechanism of excess conductivity and PG formation in $Y_{1-x}Cd_xBa_2Cu_3O_{7-\delta}$, with $x = 0$, 0.1, 0.3, and 0.4 (samples Y1, Y2, Y3 and Y4). It is shown that with an increase in x, the resistivity of the samples ρ increases noticeably, and the critical temperature of the transition to the superconducting state T_c decreases. It is found that the dependence $\rho(T)$ at $x = 0$ is not linear, but $\rho(T) \sim T^2$, which is typical for overdoped cuprates. Most likely, this type of ρ (T) curve is a specific feature of the studied polycrystalline sample. Fluctuation conductivity is determined by analyzing excess conductivity σ'(T) in Y1–Y4, in the $T_c^{mf} < T < T_{01}$ temperature range. It is shown that near T_c, the fluctuation conductivity is well described within the framework of the 3D Aslamazov–Larkin (AL) fluctuation theory. Above the temperature of the 3D–2D crossover, $T_0 < T_{01}$, the 2D–AL theory is applicable. In samples Y1, Y2, and Y4, the 2D Maki–Thompson (MT) contribution is not detected, which indicates the presence of defects in the studied polycrystalline samples. Sample Y3 with $x = 0.3$ is eliminated from the overall scenario, as it exhibits weak 2D–MT fluctuations above T_0, indicating a somewhat unexpected improvement in the structure of the sample. This is also supported by the shape of the PG dependence, $\Delta^*(T)$, which is typical for optimally doped YBCO single crystals with a pronounced minimum at T_{01} and a maximum at T_0, near T_c. Accordingly, the value of the PG in Y3, $\Delta^*(T_G)/k_B = 223.2$ K, is noticeably larger than $\Delta^*(T_G)/k_B = 217.4$ K inY1.

With a further increase in the concentration of cadmium to $x = 0.4$ (Y4), the shape of the $\Delta^*(T)$ curve (Fig. 7) changes again. In this case, T^*, T_{pair}, and $\Delta^*(T_{pair})$ decrease noticeably (Table II), and the maximum at T_0 and the minimum at T_{01} disappear. At the same time, $\Delta^*(T_G)/k_B$ increases to ~224.4 K (Table II). It can be assumed that doping with Cd creates an internal pressure in YBCO, which leads to the observed increase in $\Delta^*(T_G)/k_B$, as a result of structural defects. This is also supported by a sharp increase in the distance d_{01} between the CuO_2 conducting planes, as determined by analyzing the fluctuation conductivity. According to the data given in Table I, it can be seen that d_{01} more than doubles with an increase in the Cd content from $x = 0$ to 0.4. However, as a whole, the change in the sample parameters with increasing x is nonmonotonic. Therefore, it can be noted that various defect ensembles arising as a result of Cd intercalation significantly affect the properties of the studied $Y_{1-x}Cd_xBa_2Cu_3O_{7-\delta}$ polycrystalline samples.

ACKNOWLEDGMENTS

The authors of the article are grateful to Professor A. L. Solovjov for his active participation in the discussion of the results, which made it possible to shed light on many aspects of the problem under study.

REFERENCES

[1]R. V. Vovk and A. L. Solovjov, FNT **44**, 111 (2018) [Low Temp. Phys. **44**, 81 (2018)].
[2]R. J. Cava, Science **243**, 656 (1990).
[3]M. Asta, D. de Futaine, G. Ceder, E. Salomons, and M. Kraitchman, J. Less. Common. Metals **168**, 39 (1991).
[4]R. V. Vovk, N. R. Vovk, and O. V. Dobrovolskiy, J. Low Temp. Phys. **175**, 614 (2014).
[5]R. V. Vovk, Z. F. Nazyrov, M. A. Obolenskii, I. L. Goulatis, A. Chroneos, and V. M. Pinto Simoes, J. Alloys Compd. **509**, 4553 (2011).
[6]S. V. Savich, A. V. Samoilov, R. V. Vovk, O. V. Dobrovolskiy, S. N. Kamchatna, Y. V. Dolgopolova, and O. A. Chernovol-Tkachenko, Mod. Phys. Lett. B **30**, 1650034 (2016).
[7]T. Timusk and B. Statt, Reports Prog. Phys. **62**, 61 (1999).
[8]S. Badoux, W. Tabis, F. Laliberte, G. Grissonnanche, B. Vignolle, D. Vignolles, J. Beard, D. A. Bonn, W. N. Hardy, R. Liang, N. Doiron-Leyraud, Lus Taillefer, and Crl Proust, Nature (London) **531**, 210 (2016).
[9]Ri-Ha He, M. Hashimoto, H. Karapetyan, J. D. Koralek, J. P. Hinton, J. P. Testaud, V. Nathan, Y. Yoshida, Hn Yao, K. Tanaka, W. Meevasana, R. G. Moore, D. H. Lu, S.-K. Mo, M. Ishikado, H. Eisaki, Z. Hussain, T. P. Devereaux, S. A. Kivelson, J. Orenstein, A. Kapitulnik, and Z.-X. Shen, Science **331**, 1579 (2011).
[10]R. Peters and J. Bauer, Phys. Rev. B **92**, 014511 (2016).
[11]A. L. Solovjov and A. M. Gabovich, *Superconductors—Materials, Properties and Applications. Chapter 7 Pseudogap and Local Pairs in High-Tc Superconductors* (Rijeka InTech, 2012), pp. 137.
[12]A. A. Kordyuk, Fiz. Nizk. Temp. **41**, 417 (2015) [Low Temp. Phys. **41**, 319 (2015)].
[13]T. Suzuki, T. Yamazaki, and R. Sekine, J. Mat. Sci. Lett. **8**, 381 (1989).
[14]V. N. Narozhnyi and V. N. Kochetkov, Phys. Rev. B **53**, 5856 (1996).
[15]M. Murakami, N. Sakai, and T. Higuchi, Supercond. Sci. Technol. **12**, 1015 (1996).
[16]A. L. Solovjov and V. M. Dmitriev, FNT **33**, 32 (2007) [Low Temp. Phys. **33**, 23 (2007)].
[17]R. V. Vovk, M. A. Obolenskii, A. A. Zavgorodniy, A. V. Bondarenko, and M. G. Revyakin, FNT **33**, 546 (2007) [Low Temp. Phys. **33**, 408 (2007)].
[18]L. P. Kozeev, M. Y. Kamenev, A. I. Romanenko, O. B. Anikeeva, V. E. Fedorov, *Materials of the 6th International Conference "Crystals: Growth, Properties, Real Structure, Application", September 8-12, 2003, VNIISIMS Publishing House (2003).*
[19]E. V. Yakubovich, N. N. Oleinikov, V. A. Ketsko, and I. V. Arkhangelskiy, Dokl. RAS **386**, 502 (2002).
[20]S. Kambe, G. Samukama, K. Yamaguchi, O. Ishu, I. Shime, T. Nomura, S. Ohshima, K. Okuyama, T. Itoh, H. Suematsu, and H. Yamauchi, Solid State Phys. **108**, 283 (1998).
[21]J. W. Chen and C. F. Chen, Solid State Commun. **69**, 1079 (1989).
[22]N. E. Alekseevskiy, A. V. Mitin, V. I. Nizhankovskiy, E. P. Khlybov, V. V. Evdokimova, and G. M. Kuzmichev, SFHT **2**, 40 (1989).
[23]S. A. Aliev, J. A. Baghirov, S. S. Ragimov, S. A. Huseyhov, V. M. Aliev, I. A. Ismailov, and A. S. Mechtiev, *Proc. 2nd Intern. Conf. on Rare Earth Development and Application V*, Beijing, China (1991).
[24]R. V. Vovk, Z. F. Nazyrov, M. A. Obolenskii, V. M. Pinto Simoes, M. Januszczyk, and J. N. Latosińska, Acta Physica Polonica A **120**, 512 (2011).
[25]V. M. Aliev, Transactions of Azerbaijan National Academy of Sciences Physics and Astronomy **32**, 110 (2012).
[26]V. M. Aliev, S. S. Ragimov, and R. I. Selim-zade, FNT **39**, 635 (2013) [Low Temp. Phys. **39**, 493 (2013)].
[27]S. A. Aliev, S. S. Ragimov, and V. M. Aliev, Azerbaijan J. Phys. **10**(4), 42 (2004).
[28]V. M. Aliev, S. A. Aliev, S. S. Ragimov, G. J. Sultanov, and B. A. Tairov, FNT **37**, 351 (2011) [Low Temp. Phys. **37**, 273 (2011)].
[29]Y. D. Tretyakov and E. A. Goodilin, UFN **69**, 1 (2000).
[30]A. Gudilin, A. P. Soloshenko, V. V. Lennikov, A. V. Knot'ko, D. A. Vetoshkin, N. N. Oleinikov, and Y. D. Tretyakov, ZNH **45**, 917 (2000).
[31]R. Fehrenbacher and T. M. Rice, Phys. Rev. Lett. **70**, 3471 (1993).
[32]A. L. Solovjov, L. V. Omelchenko, R. V. Vovk, and S. N. Kamchatnaya, FNT **43**, 1050 (2017) [Low Temp. Phys. **43**, 841 (2017)].
[33]G. D. Chryssikos, E. I. Kamitsos, J. A. Kapoutsis, A. P. Patsis, V. Psycharis, A. Kafoudakis, C. Mitros, G. Kallias, E. Gamari-Seale, and D. Niarchos, Physica C **254**, 44 (1995).
[34]S. Hikami and A. I. Larkin, Mod. Phys. Lett. B **2**, 693 (1988).
[35]M. Randeria, Nat. Phys. **6**, 561 (2010).
[36]I. Esterlis, S. A. Kivelson, and D. J. Scalapino, Phys. Rev. B **44**, 174516 (2019).
[37]Y. Ando, S. Komiya, K. Segawa, S. Ono, and Y. Kurita, Phys. Rev. Lett. **93**, 267001 (2004).
[38]E. V. L. de Mello, M. T. D. Orlando, J. L. Gonzalez, E. S. Caixeiro, and E. Baggio-Saitovich, Phys. Rev. B **66**, 092504 (2002).
[39]A. L. Solovjov, L. V. Omelchenko, V. B. Stepanov, R. V. Vovk, H.-U. Habermeier, H. Lochmajer, P. Przyslupski, and K. Rogacki, Phys. Rev. B **94**, 224505 (2016).
[40]M. S. Grbić, M. Požek, D. Paar, V. Hinkov, M. Raichle, D. Haug, B. Keimer, N. Barčić, and A. Dulčić, Phys. Rev. B **83**, 144508 (2011).
[41]W. Lang, G. Heine, W. Kula, and R. Sobolewski, Phys. Rev. B **51**, 9180 (1995).
[42]B. P. Stojkovic and D. Pines, Phys. Rev. B **55**, 8576 (1997).
[43]H. Alloul, T. Ohno, and P. Mendels, Phys. Rev. Lett. **63**(16), 1700 (1989).
[44]T. Kondo, A. D. Palczewsk, Y. Hamaya, T. Takeuchi, J. S. Wen, Z. J. Xu, G. Gu, and A. Kaminski, Phys. Rev. Lett. **111**, 157003 (2013).
[45]B. Oh, K. Char, A. D. Kent, M. Naito, M. R. Beasley, T. H. Geballe, R. H. Hammond, J. M. Graybeal, and A. Kapitulnik, Phys. Rev. B **37**, 7861 (1988).
[46]P. G. De Gennes, Superconductivity of Metals and Alloys (W. A. Benjamin, INC., New York–Amsterdam, 1966), p. 280.
[47]A. Kapitulnik, M. R. Beasley, C. Castellani, and C. Di Castro, Phys. Rev. B **37**, 537 (1988).
[48]Y. B. Xie, Phys. Rev. B **46**, 13997 (1992).
[49]A. I. Dyachenko, V. Y. Tarenkov, S. L. Sidorov, V. N. Varyukhin, and A. L. Solovjov, FNT **39**, 416 (2013) [Low Temp. Phys. **39**, 323 (2013)].
[50]V. J. Emery and S. A. Kivelson, Nature (London **374**, 434 (1995).
[51]J. Corson, R. Mallozzi, J. Orenstein, J. N. Eckstein, and I. Bozovic, Nature (London) **398**, 221 (1999).
[52]A. L. Solovjov and V. M. Dmitriev, FNT **32**, 139 (2006) [Low Temp. Phys. **32**, 99 (2006)].
[53]A. L. Solovjov and V. M. Dmitriev, FNT **35**, 227 (2009) [Low Temp. Phys. **35**, 169 (2009)].
[54]B. Leridon, A. Defossez, J. Dumont, J. Lesueur, and J. P. Contour, Phys. Rev. Lett. **87**, 197007 (2001).
[55]D. D. Prokofiev, M. P. Volkov, and Y. A. Boykov, FTT **45**, 1168 (2003).
[56]Y. Yamada, K. Anagawa, T. Shibauchi, T. Fujii, T. Watanabe, A. Matsuda, and M. Suzuki, Phys. Rev. B **68**, 054533 (2003).
[57]J. Stajic, A. Iyengar, K. Levin, B. R. Boyce, and T. R. Lemberger, Phys. Rev. B **68**, 024520 (2003); D. S. Inosov, J. T. Park, A. Charnukha, Ya Li, A. V. Boris, B. Keimer, and V. Hinkov, Phys. Rev. B **83**, 214520 (2011).
[58]Ø. Fischer, M. Kugler, I. Maggio-Aprile, and C. Berthod, Rev. Mod. Phys. **79**, 353 (2007).
[59]A. L. Solovjov, E. V. Petrenko, L. V. Omelchenko, R. V. Vovk, I. L. Goulatis, and A. Chroneos, Sci. Rep. **9**, 9274 (2019).
[60]R. Haussmann, Phys. Rev. B **49**, 12975 (1994).
[61]J. R. Engelbrecht, A. Nazarenko, M. Randeria, and E. Dagotto, Phys. Rev. B **57**, 13406 (1998).

[62]V. P. Gusynin, V. M. Loktev, and S. G. Sharapov, JETP Lett. **65**(2), 170 (1997).
[63]A. L. Solovjov, L. V. Omelchenko, R. V. Vovk, O. V. Dobrovolskiy, S. N. Kamchatnaya, and D. M. Sergejev, Curr. Appl. Phys. **16**, 931 (2016).
[64]A. L. Solovjov, L. V. Omelchenko, E. V. Petrenko, R. V. Vovk, V. V. Khotkevych, and A. Chroneos, Sci. Rep. **9**, 20424 (2019).

Translated by AIP Author Services